© 2014. Published by The Company of Biologists Ltd | Development (2014) 141, 1313-1323 doi:10.1242/dev.104646

RESEARCH ARTICLE

Ontogeny, conservation and functional significance of maternally inherited DNA methylation at two classes of non-imprinted genes

Charlotte E. Rutledge[1,*,‡], Avinash Thakur[1,‡], Karla M. O'Neill[1], Rachelle E. Irwin[1], Shun Sato[2], Ken Hata[2] and Colum P. Walsh[1,§]

ABSTRACT

A functional role for DNA methylation has been well-established at imprinted loci, which inherit methylation uniparentally, most commonly from the mother via the oocyte. Many CpG islands not associated with imprinting also inherit methylation from the oocyte, although the functional significance of this, and the common features of the genes affected, are unclear. We identify two major subclasses of genes associated with these gametic differentially methylated regions (gDMRs), namely those important for brain and for testis function. The gDMRs at these genes retain the methylation acquired in the oocyte through preimplantation development, but become fully methylated postimplantation by *de novo* methylation of the paternal allele. Each gene class displays unique features, with the gDMR located at the promoter of the testis genes but intragenically for the brain genes. Significantly, demethylation using knockout, knockdown or pharmacological approaches in mouse stem cells and fibroblasts resulted in transcriptional derepression of the testis genes, indicating that they may be affected by environmental exposures, in either mother or offspring, that cause demethylation. Features of the brain gene group suggest that they might represent a pool from which many imprinted genes have evolved. The locations of the gDMRs, as well as methylation levels and repression effects, were also conserved in human cells.

KEY WORDS: Epigenetics, DNA methylation, Imprinting

INTRODUCTION

DNA methylation in mammals refers to the modification of cytosine by the addition of a methyl group, usually at the CpG dinucleotide. Because methylcytosine spontaneously deaminates at very high frequency, methylated cytosines are lost from the germline genome (Walsh and Xu, 2006; Weber et al., 2007), resulting in under-representation except at CpG islands (CGIs). These are normally unmethylated and under strong selective pressure to remain so. CGIs are sometimes classed as 'weak' or 'strong', depending on the CpG density and are frequently associated with the transcriptional start sites of genes (Deaton and Bird, 2011). Classically, CGIs have been identified by bioinformatic means but, more recently, biochemical assays based on binding of the CXXC domain protein CFP1 have been used to identify CGIs conserved between mouse and human, almost half of which were not detected bioinformatically. Many CFP1-defined CGIs are located away from annotated promoters in intra- or intergenic locations, and have been termed 'orphan' CGIs (Illingworth et al., 2010).

Although genome-wide sequencing approaches have increased our knowledge of when and where methylation occurs, relatively few classes of genes have been demonstrated to be functionally regulated by methylation. One group of developmentally important genes demonstrably controlled by methylation consists of imprinted genes (Bartolomei and Ferguson-Smith, 2011). These are associated with gametic differentially methylated regions (gDMRs), which show different levels of methylation in sperm and egg, driven by the activity of the *de novo* enzyme DNA methyltransferase 3A (DNMT3A) and the essential co-factor DNMT3L (Shirane et al., 2013), but with a possible small contribution from DNMT3B in sperm (Kaneda et al., 2004). Loss of differential methylation causes changes in transcription at the imprinted genes. Methylation of imprinted gDMRs largely occurs (19/22 gDMRs) in the oocyte (Reik and Walter, 2001; Proudhon et al., 2012).

Methylation patterns differ globally between the gametes, not just at imprinted regions, and many non-imprinted loci have recently been shown to have gDMRs (Kobayashi et al., 2012; Smallwood et al., 2011). Following fertilisation, almost total erasure occurs on the paternally inherited chromosomes however, probably mediated by TET3 (Gu et al., 2011). For maternal chromosomes too there is a passive loss of methylation by dilution, until it reaches a minimum at the blastocyst stage. Following implantation *de novo* methylation occurs, primarily driven by DNMT3B (Borgel et al., 2010). DNMT3 family members are barely detectable in most adult tissues except testis and thymus, although DNMT3A is also found in brain (Okano et al., 1999; Wu et al., 2010; Xu et al., 1999). Thus, propagation of methylation patterns is thought to be reliant on the ubiquitous maintenance enzyme DNMT1 (Howell et al., 2001; Li et al., 1992), although DNMT3A/B may also play a role in embryonic stem cells (ESCs) (Chen et al., 2003).

Despite some recent studies looking at loci inheriting methylation from the mother (Borgel et al., 2010; Smallwood et al., 2011; Kobayashi et al., 2012), a number of questions remain unresolved. In particular, we aimed to: (1) determine if there are any gene classes that are over-represented in these ~1000 oocyte-specific gDMRs; (2) determine the functional significance of methylation at these loci by removing it and examining the transcriptional response; (3) examine the conservation of any gDMR between human and mouse; (4) determine the methyltransferases important for establishment and maintenance of the gDMR; and (5) compare the gDMR properties with those of imprinted loci.

[1]Centre for Molecular Biosciences, School of Biomedical Sciences, University of Ulster, Coleraine BT52 1SA, UK. [2]Department of Maternal-Fetal Biology, National Research Institute for Child Health and Development, 2-10-1 Okura, Setagaya, Tokyo 157-8535, Japan.
*Present address: Journal of Cell Science, The Company of Biologists, 140 Cowley Road, Cambridge CB4 0DL, UK.
‡These authors contributed equally to this work

§Author for correspondence (cp.walsh@ulster.ac.uk)

Received 8 October 2013; Accepted 2 January 2014

Development (2014) doi:10.1242/dev.104646

We show here that there are three distinct types of oocyte gDMR: those associated with imprinted genes and then two transient gDMR classes, one containing genes associated with testis function and the other with brain function. The former appear to be marked at the promoter by DNA methylation, helping to suppress transcription. The brain-specific genes are instead methylated intragenically. Postfertilisation, both testis and brain gDMRs become fully methylated by *de novo* methylation of the paternal allele. Testis-specific genes require methylation for complete repression, and in its absence they become upregulated by several orders of magnitude. Unlike imprinted genes, neither of the non-imprinted gDMR classes requires germline passage to re-establish methylation.

RESULTS

Identification of genes that resemble imprinted genes in their methylation ontogeny

We reanalysed recently published (Kobayashi et al., 2012; Smallwood et al., 2011) datasets looking for CGIs that: (1) were completely methylated (>75%) in wild-type (WT) meiosis II (MII) oocytes; (2) were significantly methylated in blastocysts; and (3) lost >50% methylation in DNMT3L-deficient oocytes. The threshold for significant methylation in blastocysts was set to 25%, based on the fact that many imprinted CGIs show methylation at ~30% in the genome-wide analyses. In the first of these studies, which used reduced representation bisulfite sequencing (RRBS) of oocytes in MII, 2146 /23,019 CGIs examined were >75% methylated in oocyte: after removing intergenic CGIs and accounting for multiple CGIs associated with a single gene, this gave 897 RefSeq-annotated genes with at least one completely methylated CGI (Fig. 1A). None of these was methylated in sperm. In blastocyst, only 529 genes had CGIs with significant methylation (Fig. 1A). Interestingly, most genes (421/529, 80%) that were methylated at this level in blastocyst were also methylated in oocyte, and more heavily methylated in oocyte than in sperm, indicating that they are oocyte gametic differentially methylated regions (oocyte gDMRs). Although we distinguish (Fig. 1A) between CGIs that appear to gain methylation preimplantation (108/529) and those that retain methylation from the oocyte (421/529), it is possible that some in the latter group are both demethylated early on and then remethylated to a lower degree on both alleles. In contrast to the oocyte CGIs, only 12 sperm gDMRs showed retention of methylation in the blastocyst. Indicating the importance of DNMT3L, 91% (382/421) of the genes methylated in both oocyte and blastocyst lost >50% of their methylation in oocytes from *Dnmt3l*$^{-/-}$ females (Fig. 1A).

To determine whether any gene class was over-represented in this group (n=382) of DNMT3L-dependent oocyte gDMR genes, we used the functional annotation clustering tool on the DAVID platform (Huang et al., 2009). The top-scoring groups of genes identified as being enriched are indicated in Fig. 1Bi. This identified genes associated with the term ‘brain’, such as *Crocc*, *Grin3b* and *Adcy6* (total n=199), as markedly over-represented (P=5.76×10^{-11}), accounting for 52% of the total group: indeed, 4/5 top classes were central nervous system genes (Fig. 1Bi). DAVID analysis of the genes methylated in blastocyst (n=529) gave very similar results. Analysis of an independent dataset derived from whole bisulfitome DNA amplification-sequencing (WBA-seq) on germinal vesicle (GV) stage oocytes (Kobayashi et al., 2012) was a close match, with identity in 4/5 classes and similar ranking despite the different approaches, stage of maturity and numbers of CGIs examined (Fig. 1Bii). By contrast, a study by Weber and colleagues employing methylated DNA immunoprecipitation (meDIP) (Borgel et al., 2010) found that the class of genes most significantly associated (P=5.6×10^{-5}) with preimplantation methylation was the testis-specific genes (Fig. 1Biii) and that some of these were oocyte gDMRs. This is likely to be due in part to differences in technique, since only promoter regions were examined in the meDIP study, and many of the testis genes had non-CGI promoters and thus were under-represented in the other studies. Examination of the WGA-seq analysis, however, also indicated that many testis-specific genes were methylated in oocyte (Kobayashi et al., 2012), despite not being highlighted by ontogeny analysis. Re-inspection confirmed that testis-specific genes, such as *Dpep3*, *Piwil1*, *Fkbp6*, *Rhox13*, *Trim52*, *Spag1*, *Ggn1*, *Tbpl1*, *Spata16*, *Csnka2ip* and *Tssk2*, identified in these two latter studies, do fulfil our criteria for DNMT3L-mediated programming. Notably, the testis-specific genes showed no overlap with the group of germline genes that are methylated postimplantation by DNMT3B, such as *Dazl*, *Sycp3* and *Tex12*, identified earlier (Borgel et al., 2010; Hackett et al., 2012; Maatouk et al., 2006; Weber et al., 2007). The latter group is completely unmethylated in oocyte and blastocyst, unlike the testis gDMR genes, is independent of DNMT3L status but dependent on DNMT3B and contains genes expressed in oocyte as well as testis (e.g. the Sycp genes).

The top-scoring class from our DAVID analyses includes a few known imprinted genes expressed in brain (e.g. *Snrpn*, *Gnas* and *Ncdn*, which were excluded from this group in later analyses), suggesting the presence of novel imprinted genes. Many new brain-specific imprinted genes were recently reported from genome-wide analyses (Gregg et al., 2010a; Gregg et al., 2010b), although only a fraction have been independently validated (DeVeale et al., 2012). Likewise, some of the testis-specific genes show allele-specific methylation preimplantation (Borgel et al., 2010), a feature of imprinted genes. Fig. 1C shows little overlap, however, between the genes identified in those studies and the brain genes identified in the RRBS dataset. Of the novel brain-specific imprinted genes identified by others, only three (*Ccdc40*, *Cdh15* and *Herc3*; Fig. 1C) also have a DNMT3L-dependent gDMR: significantly, these are among the minority that have been experimentally validated (DeVeale et al., 2012; Gregg et al., 2010a; Proudhon et al., 2012). Our analysis therefore suggested that there might be three classes of DNMT3L-programmed gDMR: those associated with imprinted genes, genes important for brain function and genes that are specific to the testis.

Fig. 1D tracks the methylation ontogeny of each of the three classes, as well as the germline genes methylated postimplantation, based on approximately equal numbers of genes representative of each class for which data are available from more than one study. All three gDMR groups show strong dependence on DNMT3L in oocyte, lower methylation in sperm and retention of methylation in blastocyst (Fig. 1D). By contrast, the postimplantation group shows no methylation at any of these stages. The brain gDMR displays higher methylation in sperm and greater variability overall than the other two groups (Fig. 1D). The CGI structure and location also differ between groups. The gDMRs of the testis genes are: (1) generally the only CGI present; (2) classical CGIs; and (3) always located at the proximal promoter position upstream of the first exon (e.g. *Rhox13*; Fig. 1E). By contrast, the brain gene had: (1) multiple CGIs; (2) gDMRs that were always intragenic CGIs, usually in an exon; (3) gDMRs that were non-classical or orphan CGIs, as defined by CFP1 binding; and (4) an unmethylated promoter CGI (e.g. *Crocc* CGI 4-1220; Fig. 1E). Confirming that brain gDMRs are largely intragenic rather than promoter associated, only 14% (21/151) of brain gDMRs common to both the RRBS and WGA-seq studies were at annotated RefSeq transcription start sites (TSSs) (Fig. 1F). Furthermore, only 18% (23/130) of the remainder were enriched for hypophosphorylated RNA polymerase II and H3K4me3, indicative of TSSs (Illingworth et

Development (2014) doi:10.1242/dev.104646

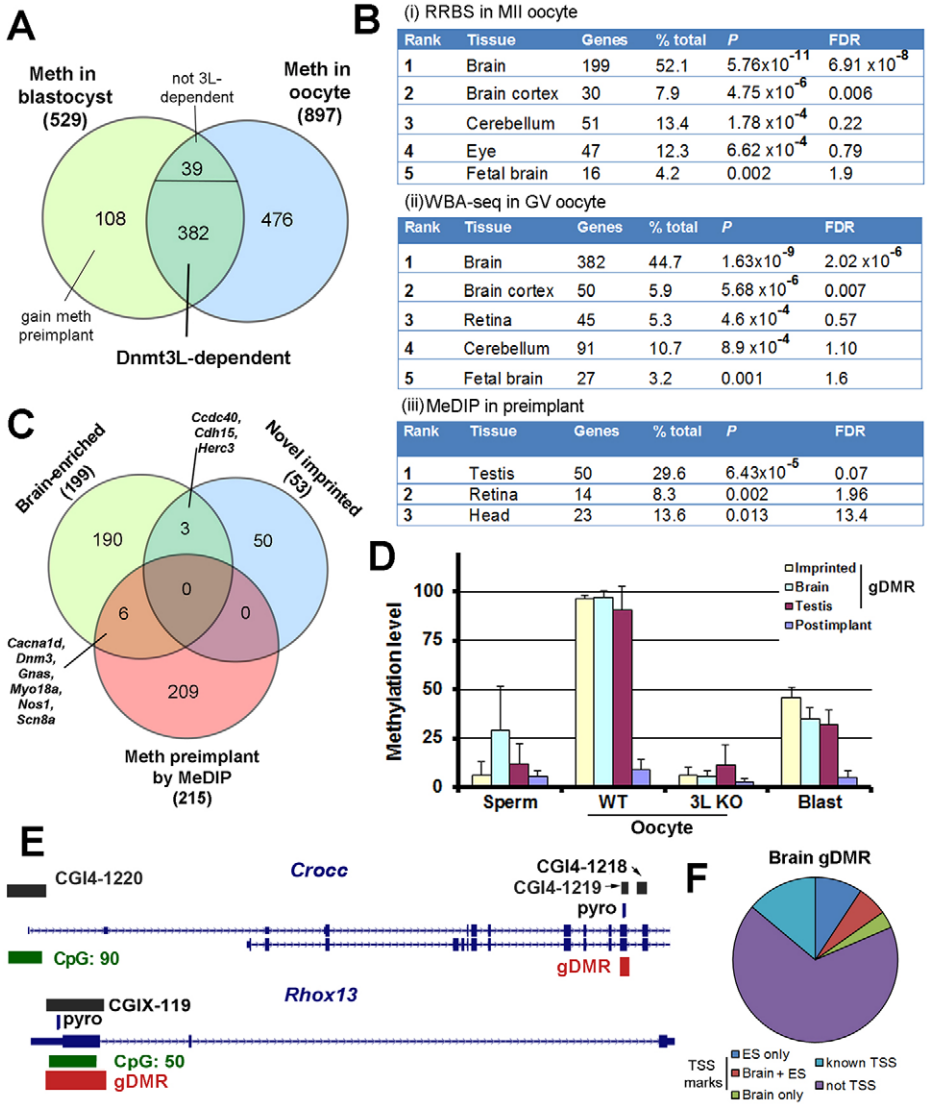

Fig. 1. Two novel gene classes with gametic differentially methylated regions (gDMRs). (A) Numbers of genes (*n*) showing methylation (Meth) in oocyte, blastocyst or both from reanalysis of published genome-wide data (Smallwood et al., 2011). DNMT3L-dependent: genes with >50% loss of methylation in DNMT3L-deficient oocytes. (B) Top-ranking classes of genes by ontology analysis of data from: (i) reduced representation bisulfite sequencing (RRBS) in meiosis II (MII) oocytes (as in A); (ii) whole bisulfitome amplified DNA sequencing on germinal vesicle (GV) oocytes [WBA-seq (Kobayashi et al., 2012)]; and (iii) methylated DNA immunoprecipitation (meDIP) on preimplantation embryos (Borgel et al., 2010). *P*-value and false discovery rate (FDR) are indicated. (C) Top-scoring class from B(i) compared with novel imprinted genes (De Veale et al., 2012) and those identified by meDIP [B(iii)]. (D) Methylation ontogeny of representative groups of genes from each gDMR class; genes methylated postimplantation are also shown as a control. 3L KO, oocytes from *Dnmt3l*$^{-/-}$ females; Blast, blastocyst. Error bars represent s.e.m. (E) Structure of prototypical brain (*Crocc*) and testis (*Rhox13*) gDMR genes. Black boxes: CpG islands (CGIs), with ID number, identified by CFP1 binding (Illingworth et al., 2010). Green boxes: CGI identified by conventional means, with number of CpGs indicated. Pyro, region covered by pyrosequencing assay. (F) Proportions of brain gDMRs at known (RefSeq) transcriptional start sites (TSSs), those showing TSS-associated chromatin marks in ESCs or brain cells, and those with no evidence of being TSSs.

al., 2010), in mouse ESCs: in brain tissues this number fell to 11% (14/130). The imprinted regions are more diverse but, as previously noted (Chotalia et al., 2009), the gDMR is generally one of multiple CGIs at these loci and tends to be intragenic. These results identify three distinct classes of gDMR programmed by DNMT3L in the mouse oocyte.

Dnmt3l is required for methylation and repression of some testis genes in the female germline

We set about validating these bioinformatic data by collecting oocytes from 22 days postpartum (22 dpp) WT and *Dnmt3l*$^{-/-}$ mice. Using combined bisulfite treatment and restriction analysis (COBRA), which produces digested bands only if a region is methylated, we first confirmed the known DNMT3L-dependent methylation of the gDMR at *Snrpn*, as a control, using oocytes from WT and *Dnmt3l*$^{-/-}$ females (Fig. 2A). *H19* shows no methylation, confirming the lack of somatic cell contamination (Fig. 2A). The testis gDMR at *Dpep3* and *Piwil1*, previously identified by meDIP (Borgel et al., 2010), also showed near-complete methylation in WT oocytes, further confirmed by clonal analysis (Fig. 2A,B). The weak CGI at *Csnka2ip*, however, only showed partial methylation in oocyte (Fig. 2A,B). Sperm methylation was seen only at the control locus *H19* (Fig. 2A). The gDMRs all showed total loss of methylation in oocytes from *Dnmt3l*$^{-/-}$ females (Fig. 2A), as confirmed by bisulfite sequencing (examples in Fig. 2B). Two further testis-specific genes, *Rhox13* and *Fkbp6*, identified by RRBS (Smallwood et al., 2011), were also highly methylated in oocyte, whereas *Dazl*, which is methylated postimplantation by DNMT3B (Weber et al., 2007), was not (Fig. 2C). Methylation at *Fkbp6* in sperm (Fig. 2C) is in contrast to earlier reports, but was confirmed by clonal analysis (supplementary material Fig. S1). *Fkbp6* is transcribed in spermatogonial stem cells (Fig. 2D) but is switched off and presumably methylated as cells enter meiosis. By contrast, *Ddx4*, which belongs to the postimplantation group, is transcribed in postmeiotic spermatocytes (white arrowhead, Fig. 2D) and not methylated in sperm.

We used pyrosequencing, a more quantitative method, to extend our studies to brain gDMRs, as these show smaller differences in methylation between sperm and oocyte (Fig. 1D). This assay gave similar results to previous COBRA and clonal analyses for imprinted (*Peg1*) and testis-specific (*Rhox13*) loci and confirmed that intragenic gDMRs at brain-specific genes such as *Grin3b*, *Adcy6* and *Crocc* show significantly different methylation between oocytes and sperm (Fig. 2E).

In order to determine if demethylation of any of these sequences results in transcriptional activation, we examined mRNA levels in ovary by reverse-transcription quantitative PCR (RT-qPCR). This

Development (2014) doi:10.1242/dev.104646

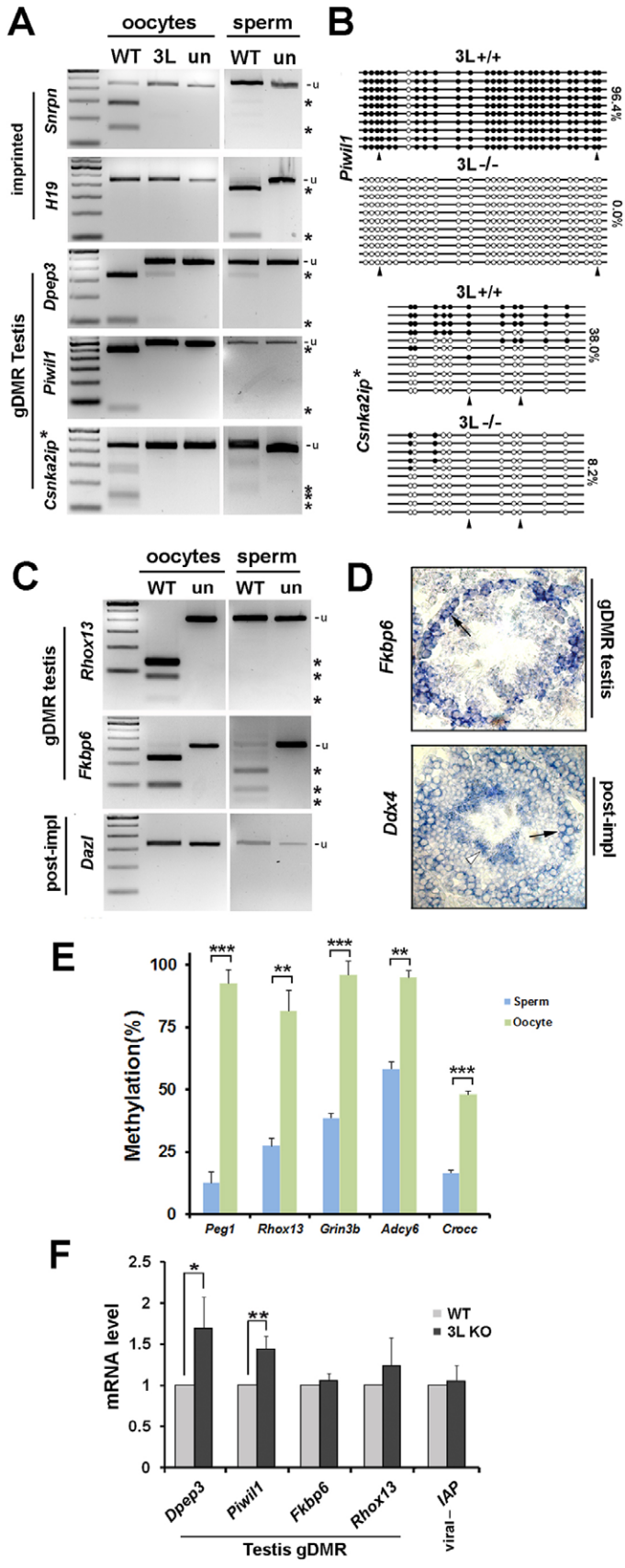

Fig. 2. Validation of methylation at novel gDMRs in gametes and effects of DNMT3L loss. (A) COBRA of methylation in wild-type (WT) and DNMT3L-deficient (3L) mouse oocytes. un, uncut; u, unmethylated; asterisk, limit digest band. (B) Clonal analysis, with methylation as a percentage of all sites indicated. Arrowheads indicate sites also analysed by COBRA. (C) As for A. Post-impl, genes known to be methylated only after implantation. (D) *In situ* hybridisation of testis tissue. Arrow indicates spermatogonial stem cells; arrowhead indicates spermatozoa. (E) Methylation of gDMRs as detected by pyrosequencing in sperm and oocytes. (F) RT-qPCR showing transcript levels in WT and 3L KO ovaries for the indicated genes. Error bars indicate s.e.m. $^{**}P<0.01$, $^{***}P<0.001$ by *t*-test.

showed a small but significant upregulation of *Dpep3* and *Piwil1* in DNMT3L-deficient ovaries (Fig. 2F), the latter supporting a previous observation (Kobayashi et al., 2012). By contrast, *IAP* was not derepressed in this tissue (Fig. 2F), despite showing levels of methylation in *Dnmt3l*$^{-/-}$ oocytes as low as those seen in primordial germ cells, where they reach their minimum (supplementary material Fig. S2). As the brain gDMRs are not at promoters, they were not assessed. These results validate the bioinformatic analysis above and suggest a role for methylation in maintaining suppression at some non-imprinted loci in oocyte.

Brain and testis gDMRs become fully methylated postimplantation, with methylation required for suppression of testis genes

When we looked at postimplantation tissues, the *Snrpn* gDMR, as expected for an imprinted gene, retained ~50% methylation in adult somatic tissues (Fig. 3A). By contrast, all of the testis gDMRs showed complete or near-complete methylation (Fig. 3A), indicating a gain of methylation on the paternal allele. Methylation levels were comparable to those seen at *Sycp3* (Fig. 3A), part of the group methylated postimplantation by DNMT3B (Weber et al., 2007). Pyrosequencing confirmed these results and extended them to brain gDMRs, which also showed near-complete methylation in adult tissues (Fig. 3B), indicating that the brain and testis gDMRs show transient, rather than stable, differential methylation. The similar levels of methylation in tissues derived from all three germ layers indicate establishment early postimplantation.

Although such high methylation is inconsistent with imprinting, it could still be important for transcriptional repression. NIH 3T3 fibroblast cells showed levels of DNA methylation comparable to primary tissues for most of the genes of interest (Fig. 3A, lanes at right); treatment with the methyltransferase inhibitor 5-aza-2′-deoxycytidine (Aza) caused demethylation (Fig. 3A,C) and strong induction (Fig. 3D) of *Sycp3* and *IAP* as expected (Borgel et al., 2010; Walsh et al., 1998). All testis gDMRs showed substantial demethylation by COBRA (Fig. 3A) and pyroassay (Fig. 3C; $P<0.05$ for all genes) and were strongly induced (Fig. 3D) from almost undetectable levels in untreated fibroblasts. Extension of this analysis to cover additional testis gDMRs by RT-qPCR showed substantial derepression at some other loci (*Rhox9*, *Trim52*, *Spata16*; Fig. 3E). There was a notable gradation of response dependent on CpG density in the gDMR: out of three testis genes containing weak CGIs (*Tssk2*, *Csnka2ip*, *Dnmt3l*), only one (*Dnmt3l*) showed significant ($P=0.04$) derepression (Fig. 3D,E); this effect on *Dnmt3l* is consistent with previous reports by ourselves and others (Hu et al., 2008; O'Doherty et al., 2011). By contrast, many of the brain gDMR genes were less heavily repressed in fibroblasts and showed substantial baseline transcription by RT-PCR, using brain as a positive control (Fig. 3D). Consistent with brain gDMRs not being cryptic promoters, Aza treatment gave demethylation (all $P<0.05$) but no significant derepression, except for a slight ($P=0.036$) effect at *Adcy6* (Fig. 3D,E). These results show a postimplantation gain of methylation on the paternal allele at brain and testis gDMRs and an

Development (2014) doi:10.1242/dev.104646

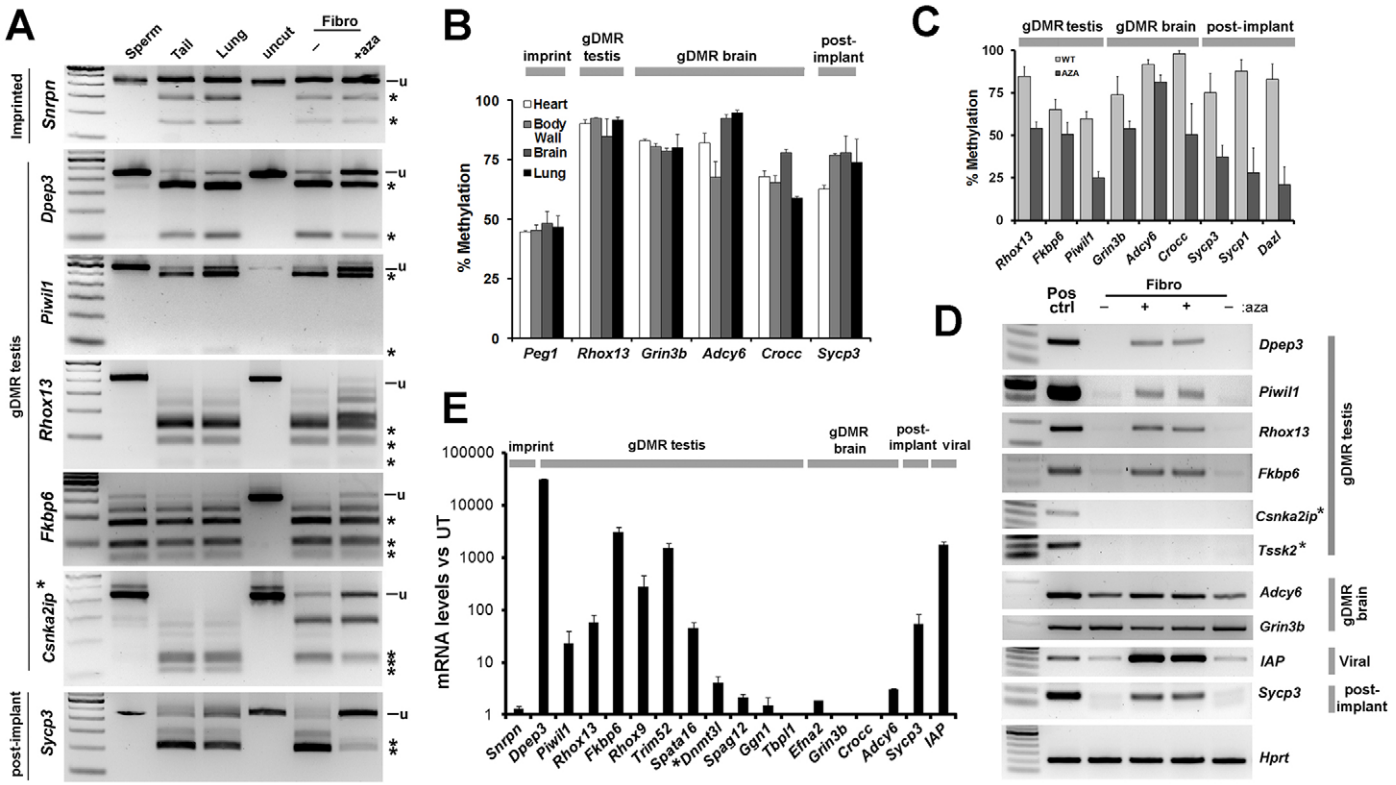

Fig. 3. Methylation and repression at novel gDMRs in adult mouse tissues. (A) COBRA on the adult mouse tissues and cell lines indicated at the top. Fibro, fibroblasts without (–) or with (+aza) 5-aza-2′-deoxycytidine. (B) Methylation analysis by pyroassay. (C) All analysed genes showed significant demethylation (P<0.05, ANOVA) by pyroassay following Aza treatment. (D) RT-PCR for the indicated genes in treated fibroblasts. Testis is a positive control (Pos ctrl), except for *Adcy6* and *Grin3b*, where brain was used. *IAP* and *Sycp3* are known to be repressed by methylation. Asterisked genes have low-density CGIs. *Hprt* is a loading control. (E) RT-qPCR of samples from D. UT, untreated. Error bars indicate s.e.m.

important role for methylation in maintaining suppression of the latter.

Conservation of methylation and repression in a human cell line

We extended our study to hTERT-1604 immortalised human fibroblasts, which have previously been shown to retain normal methylation at many loci (Loughery et al., 2011). Methylation at the *SNRPN* locus is within the 40-60% range (Fig. 4A) normal for imprinted gDMRs (Woodfine et al., 2011). The testis-specific genes *DPEP3*, *PIWIL1* and *FKBP6* showed high levels of conservation between mouse and human, retained their promoter CGIs and were heavily methylated (Fig. 4A). *SYCP3* and *DAZL* were also heavily methylated as expected, and are shown as controls (Fig. 4A). Many brain genes also showed conservation of the intragenic CGI that constitutes the murine gDMR. Methylation was >75% for *GRIN3B* and *ADCY6*, as seen in mouse, although *EFNA* was not heavily methylated in this cell line (Fig. 4A).

Contrasting with robust signal in testis, little or no transcription from the testis gDMR group (*DPEP3*, *FKBP6*, *PIWIL1*) or from the genes methylated postimplantation (*SYCP3*, *SYCP1*, *DAZL*, *TEX12*) could be detected in untreated hTERT-1604 fibroblasts, as expected (Fig. 4B). Humans lack a *Rhox13* homologue, but *RHOXF1*, which is related to the ancestral gene in mice, also showed the same expression pattern (Fig. 4B). On treatment with Aza, all of the testis loci except *FKBP6* showed significant demethylation (P<0.05; Aza, Fig. 4C), although it is notable that the gDMR appeared to be more resistant (loss <10%) than the postimplantation genes (loss >15%). All genes except *PIWIL1* were reliably upregulated (Fig. 4B) and RT-qPCR confirmed major differences in transcript levels versus control (P<0.05; Fig. 4D). Brain genes showed low-level transcription in fibroblasts and failed to show substantial upregulation with Aza (not shown), as found in mouse (Fig. 3D). Aza affects all three methyltransferases as well as having some non-specific effects, so we also carried out siRNA knockdown for *DNMT1* and collected RNA at day 4. Significant (P<0.05) demethylation at all the testis and postimplantation loci examined (siRNA, Fig. 4C) correlated with upregulation of *FKBP6*, *SYCP3* and *DAZL* (Fig. 4D). These results confirm that methylation plays an evolutionarily conserved role in regulating testis genes identified as gDMR in mice, as well as germline genes methylated postimplantation.

Contribution of DNMT1 versus DNMT3A/B to maintenance methylation of gDMRs

We used knockout (KO) ESC lines to assess the dependence of non-imprinted gDMRs on the maintenance versus *de novo* enzymes for perpetuation of methylation. Parental J1 ESCs retain appropriate methylation at the *Snrpn*, *H19* and *Peg1* gDMRs by COBRA (Fig. 5A) and/or pyrosequencing (Fig. 5D), and clonal analysis showed that *Snrpn* predominantly displays the two patterns typical of imprinted genes, either fully methylated or fully unmethylated (Fig. 5B). J1 ESCs lacking a functional *Dnmt1* gene also showed methylation loss at the imprinted loci, as expected (1KO, Fig. 5A,D). Whereas all of the testis gDMRs showed levels of methylation comparable to (*Piwil1*, *Rhox13*, *Fkbp6*) or greater than

Development (2014) doi:10.1242/dev.104646

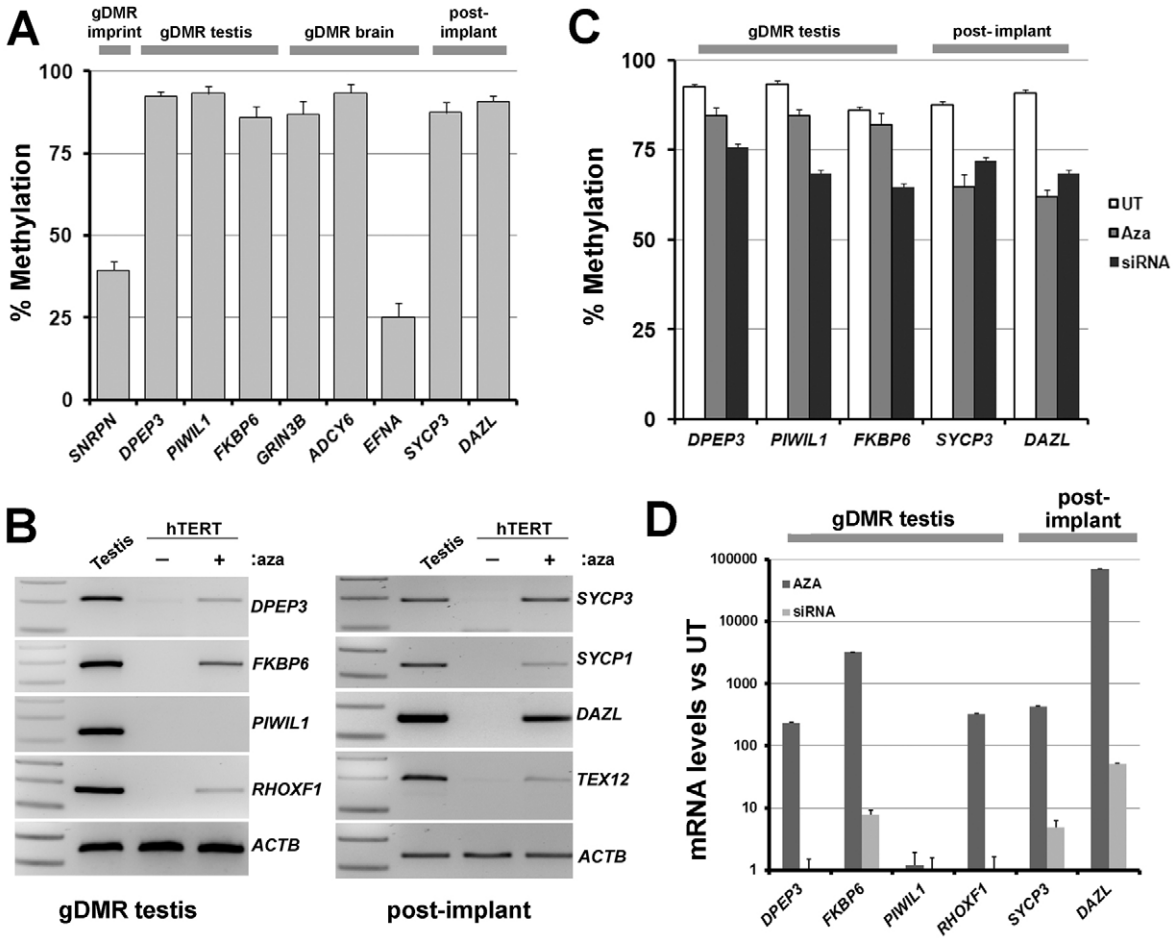

Fig. 4. Conservation of methylation and repression in human. (A) Methylation levels as determined by pyrosequencing in hTERT-1604 normal human fibroblasts. (B) RT-PCR showing derepression by Aza treatment (lane +) is comparable between testis gDMR genes (left) and genes methylated postimplantation (right). Adult testis is a positive control; *ACTB* is for loading. (C) Significant differences in methylation were seen at all analysed genes in cells exposed to Aza or depleted of DNMT1 by siRNA (P<0.05, except for *FKBP6* with Aza which was not significant). (D) RT-qPCR for the same samples. All upregulation >5-fold was significant at P<0.05. Error bars indicate s.e.m.

(*Dpep3*, *Csnka2ip*) in blastocyst, they showed clear loss of methylation in DNMT1 KO cells by COBRA (Fig. 5A) and significant demethylation by pyroassay; *Rhox13* is shown as an example (Fig. 5D; WT versus 1KO, P=0.002). The same was true for brain gDMRs, as assessed by pyroassay (Fig. 5D; all P<0.05). Interestingly, although *Fkbp6*, like *Snrpn*, shows ~50% methylation overall there is less clear partitioning of methylation into fully methylated versus fully unmethylated alleles (Fig. 5B). The same was true for the *Grin3b* brain gDMR (Fig. 5B). We also examined methylation levels in two independent *Dnmt3a*$^{-/-}$ *Dnmt3b*$^{-/-}$ double KO (DKO) lines, 16aabb and 7aabb (Okano et al., 1999). These showed significant (P<0.05) loss of methylation at all testis and brain gDMRs except *Crocc*, as well as at the imprinted gDMRs (Fig. 5C,D). Our results confirm that, in the absence of these enzymes, methylation cannot be maintained by DNMT1 alone.

Triple KO (TKO) ESCs lacking all three DNMT enzymes have been previously reported to have 4- to 15-fold increases in *Dpep3*, *Fkbp6*, *Rhox13* and *Dazl* transcript levels and ~5-fold increases in *IAP* levels (Karimi et al., 2011b). We used RT-qPCR in WT, 1KO and 3ab DKO cells to separate the cell response to the loss of either the maintenance enzyme or the *de novo* enzyme systems. The greatest changes were seen at the *Dpep3* and *IAP* loci in both cell types, with greater derepression [10-fold (P=0.002) and 5-fold (P=0.05), respectively] in the 1KO cells (Fig. 5E). The other genes, including *Fkbp6*, which showed the largest change (15-fold) in the previous study, showed smaller but reproducible (4-fold in 3ab DKO cells, P=0.027) alterations in transcript levels (Fig. 5E). There was no significant derepression at brain gDMR genes. These results suggest that DNMT1 contributes the most to repression at these loci and that strategies aimed at inhibiting all three enzymes (such as Aza treatment) should have the greatest effect on derepression.

Non-imprinted gDMRs do not require germline passage to acquire *de novo* methylation

A number of studies have shown that imprinted gDMRs, which acquire their methylation in the growing oocyte in a *Dnmt3l*-dependent process, are unable to re-establish this methylation outside of the female germline, once lost (Chen et al., 2003; Holm et al., 2005; Tucker et al., 1996; Wernig et al., 2007). Since the brain and testis gDMRs also acquire their methylation in the oocyte we examined whether they too needed to pass through the germline for successful reprogramming. We examined methylation in 1KO ESCs rescued with a cDNA expressing full-length DNMT1 protein (1KO+1) (Oda et al., 2006). As expected, rescued cells fail to remethylate imprinted gDMRs (Fig. 6A,B; 1KO versus IKO+1, P=0.57; not significant for *Peg1*); by contrast, all testis and brain

Development (2014) doi:10.1242/dev.104646

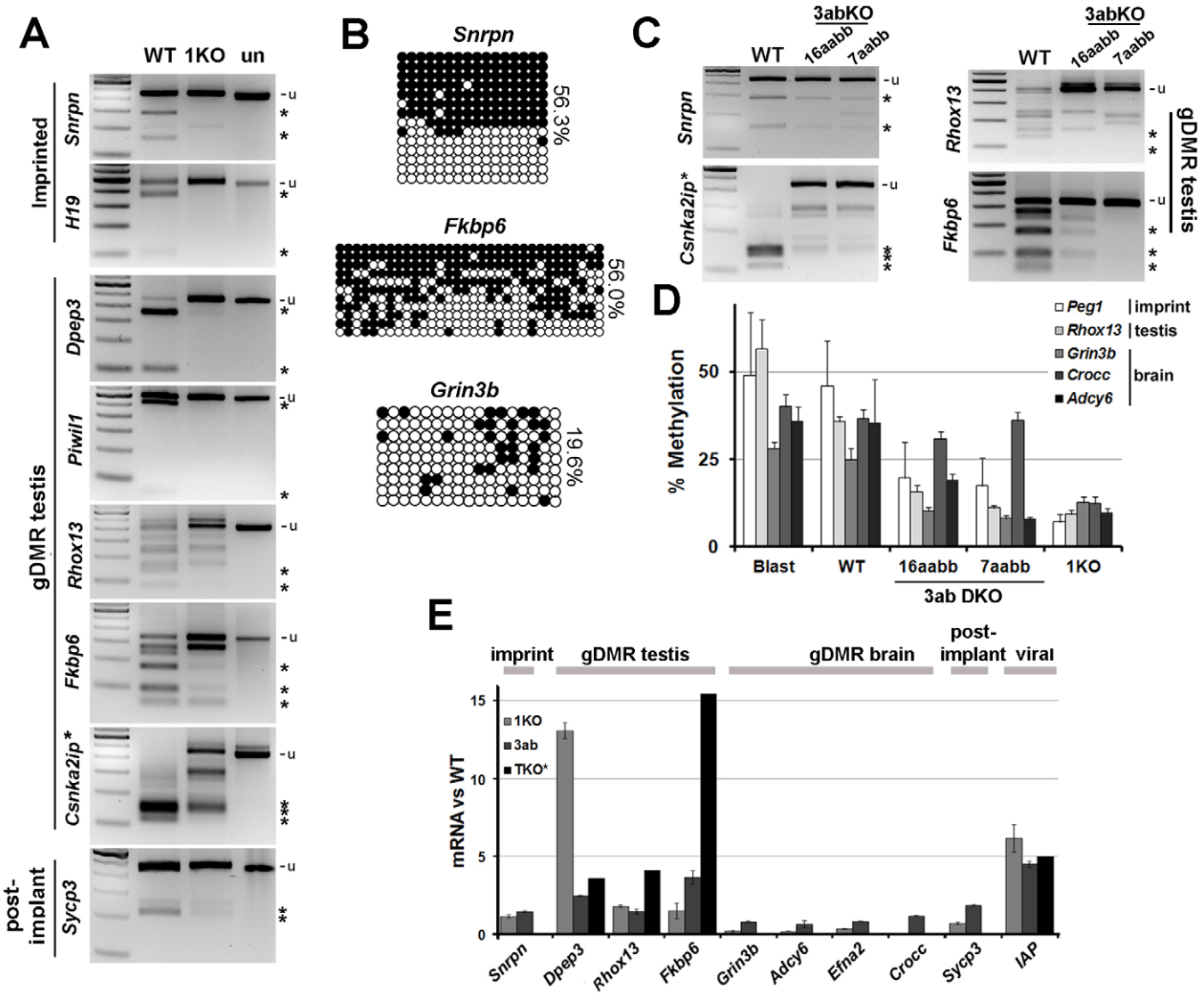

Fig. 5. Enzyme dependence for gDMR classes in mouse stem cells. (A) Methylation levels in parental J1 ESCs (WT) and DNMT1-deficient derivatives (1KO) assessed by COBRA. un, uncut control. (B) Clonal analysis of a gDMR from an imprinted, testis or brain gene (*Snrpn*, *Fkbp6* and *Grin3b*, respectively). (C) COBRA showing methylation levels in clonally derived ESCs (16aabb, 7aabb) carrying double knockouts (DKO) in both *Dnmt3a* and *Dnmt3b*. (D) Pyrosequencing for the indicated gDMRs. Blastocyst methylation levels are derived from the analysis shown in Fig. 1D. Differences between DKO and WT were significant ($P<0.05$) for all analysed genes except *Crocc*. (E) Fold reactivation in mutant versus WT cells as assessed by RT-qPCR. 3ab, DKO cells (as above); TKO, triple KO cells lacking DNMT1, DNMT3A and DNMT3B, data from Karimi et al. (Karimi et al., 2011b); brain and imprint gDMR unavailable. Error bars indicate s.e.m.

gDMRs, except *Adcy6*, showed significant gains in methylation (Fig. 6A,B; 1KO versus 1KO+1, $P<0.05$).

As methylation was not restored to WT levels, we quantitated the global increase in methylation in rescued cells using the LUMA assay (Karimi et al., 2011a), which is a bisulfite-independent quantitative assay that uses methylation-sensitive and -insensitive restriction enzyme cleavage to estimate total genomic methylation levels, and showed that 1KO+1 cells had an overall gain of 28% versus 1KO cells (Fig. 6C). As the pyroassay appeared to be showing slightly lower gains in methylation than COBRA, we also carried out clonal analysis of representative genes (Fig. 6D; supplementary material Fig. S3). Graphing these results (Fig. 6E) confirms the difference between imprinted (no significant gain, $P=1$) and non-imprinted (significant, $P<0.05$) loci, with the average increase across the four non-imprinted gDMRs being 26%, in good agreement with LUMA (Fig. 6C). In keeping with the re-establishment of repression, RT-qPCR showed that transcript levels were lower in 1KO+1 cells than in 1KO (not shown).

Levels of *de novo* methyltransferase activity in almost all adult tissues are reported to be very low (Okano et al., 1998), implying that methylation might not be restored at these non-imprinted gDMRs in adult cells. To test this, we were able to significantly deplete NIH 3T3 cells of DNMT1 using siRNA (Fig. 6F; $P=1.8\times10^{-5}$, day 4 versus scrambled control), then allowed the DNMT1 levels to recover and examined the response of the gDMR. Four days after knockdown of DNMT1 there was a decrease in methylation at all loci tested ($P<0.05$) due to loss of maintenance activity (Fig. 6G; untreated levels set to 100%), with brain gDMRs showing the greatest response. As DNMT1 levels recovered the percentage of methylated sites increased, presumably due to its maintenance activity stabilising the methylation added by the *de novo* enzymes, as in ESCs [see above and Oda et al. (Oda et al.,

Development (2014) doi:10.1242/dev.104646

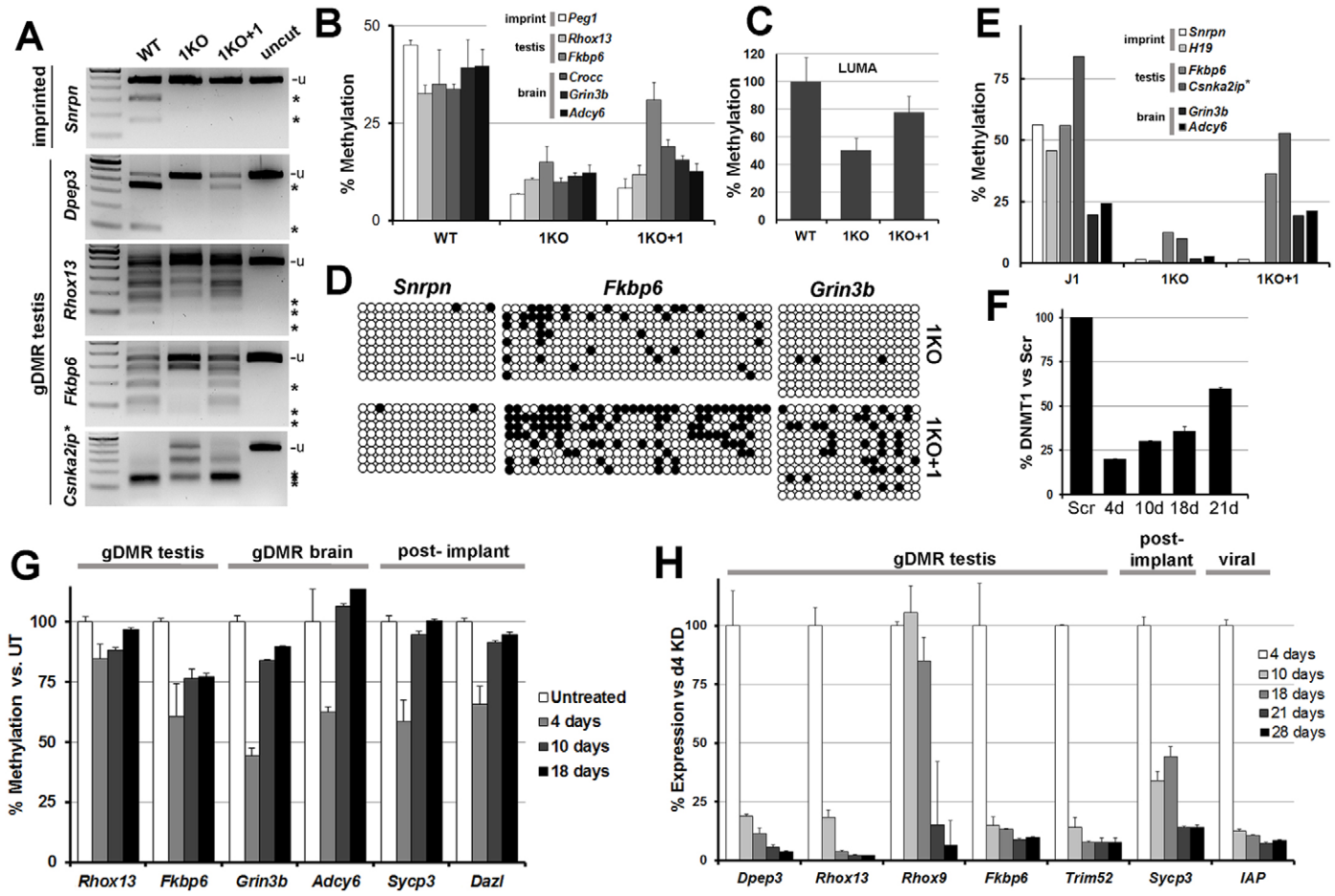

Fig. 6. Reprogramming ability of the different gDMR classes. (A) Methylation by COBRA in ESCs with normal (WT), absent (1KO) and rescued (1KO+1) DNMT1 status. (B) Pyroassay indicates significant (P<0.05) gain in methylation in 1KO+1 cells for all analysed genes except *Peg1* and *Adcy6*. (C) Overall gain in methylation in 1KO+1 cells assayed by LUMA. (D) Clonal analysis for one gene from each class of gDMR. (E) Analysis of clones indicates significant (P<0.05) gain in methylation in 1KO+1 cells for all non-imprinted genes analysed. (F) Timecourse of *Dnmt1* knockdown and recovery by RT-qPCR following transient transfection of adult mouse fibroblasts with siRNA. Scr, scrambled control; d, days. (G) Pyroassay showing methylation loss and re-establishment for samples shown in F; untreated set to 100%. All genes were significantly demethylated (P<0.05) at 4 days, but were no longer significantly different from untreated (UT) at 18 days, except for *Fkbp6*. (H) RT-qPCR of same samples showing re-establishment of repression. Day 4 values were set to 100%. KD, knockdown. Error bars indicate s.e.m.

2006)], until by 18 days there was no longer a significant difference (all P>0.05) in methylation between untreated and treated cells except at the *Fkbp6* locus, which remained demethylated (P<0.007). Examination of transcription levels showed that, following derepression (P<0.05) of testis gDMR genes at day 4 (subsequently set to 100%), the genes were silenced again rapidly (Fig. 6H).

DISCUSSION

Although a number of recent studies have identified transient gDMRs methylated in the oocyte (Borgel et al., 2010; Kobayashi et al., 2012; Proudhon et al., 2012; Smallwood et al., 2011; Smith et al., 2012), the functional significance of the methylation and the types of genes affected were not identified. We show here for the first time that transient gDMRs fall into two classes, one containing genes predominantly expressed in the testis and the other enriched in genes associated with brain function. Both groups have higher levels of methylation in the oocyte than in sperm, are very dependent on DNMT3L and retain methylation at levels of 25% or more in blastocyst (Fig. 7). Although they resemble imprinted genes in these respects, they fail to maintain differential methylation in differentiated somatic tissues due to *de novo* methylation of paternal alleles after implantation. As previously noted (Smallwood et al., 2011; Proudhon et al., 2012), this highlights protection of the unmethylated imprinted allele in the post-gastrulation embryo as one of the most important properties of imprinted loci.

The difference between a transient gDMR described here and an imprinted gDMR at a gene such as *Cdh15* is not substantial, as the latter gains methylation postimplantation on the paternal allele as well as becoming biallelically expressed in certain tissues (Proudhon et al., 2012). It has been previously noted that many imprinted genes are expressed in brain (Wilkinson et al., 2007) and have intragenic gDMRs (Smallwood and Kelsey, 2012). Since slightly more than half of all transient gDMRs are associated with brain ontologies (Fig. 1B) and are at CGIs old enough to show conservation between human and mouse (Fig. 4), it seems reasonable to speculate that some brain-specific imprinted genes might have arisen from this particular group by, for example, alterations at a transient gDMR locus that allow for protection of the paternal allele from *de novo* methylation postimplantation.

With respect to the functional significance of methylation at the transient gDMR, we show that demethylation causes transcriptional derepression of testis genes in the *Dnmt3l*$^{-/-}$ ovary, *Dnmt1*$^{-/-}$ or

Development (2014) doi:10.1242/dev.104646

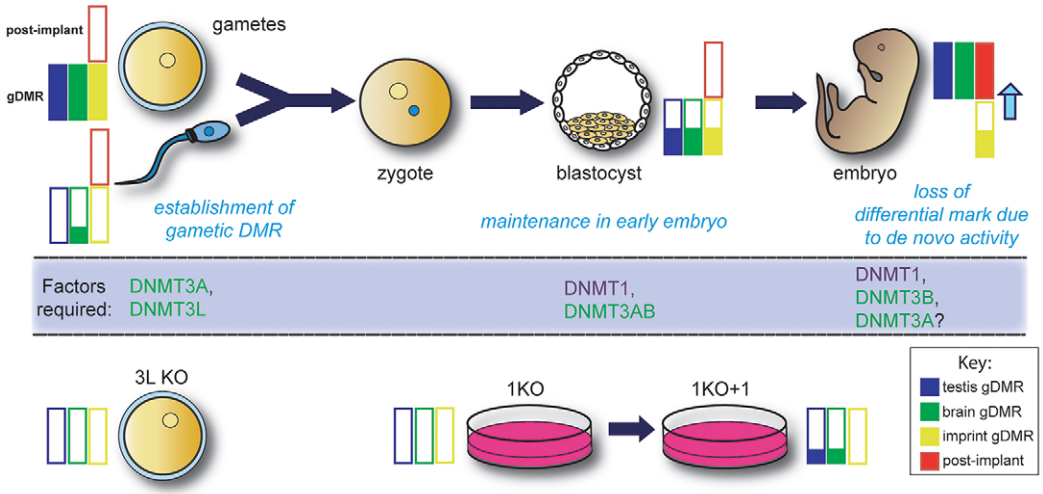

Fig. 7. Methylation dynamics and methyltransferase dependency of genes inheriting methylation from the mother. (Top) Methylation ontogeny of brain, testis and imprinted gDMRs, as well as of postimplantation genes. The average methylation of each gene class (see key, bottom right) is shown: filled bar, 100% methylation; empty bar, 0% methylation. Methyltransferase requirements at different stages, where established, are shown within the central blue panel. (Bottom) The effect of loss and restoration of methyltransferase activity in different experimental systems. The dish on the right represents ESCs.

Dnmt3ab$^{-/-}$ stem cells, and Aza-treated or *DNMT1* siRNA-treated adult cells, with the effect being much greater in the differentiated somatic cells. It is possible that methylation of the maternal allele is used to effectively halve the expression level of the transient gDMR preimplantation: however, this effect is likely to be small at this developmental stage, as derepression in KO ESCs is orders of magnitude lower than in differentiated cells. Testis genes that are regulated by a gDMR can be identified by the following characteristics: they have a high density or 'strong' CGI at the promoter, they are >75% methylated in oocytes, are DNMT3L dependent and retain methylation above 25% in blastocyst. Interestingly, although it has been suggested that intermediate density or 'weak' CGIs would be most susceptible to regulation by methylation (Borgel et al., 2010; Weber et al., 2007) we found that loss of methylation at weak CGIs could not derepress most of the genes examined: many of the loci identified by meDIP fall into this category.

Significantly, there is good conservation in humans of the CGIs that represent the gDMRs for both the testis and brain genes and they are also heavily methylated in adult tissues, which is atypical for most CGIs (Borgel et al., 2010). Conservation points to an evolutionarily conserved requirement for methylation at these loci: this is consistent with a regulatory role for the testis group, as they can be derepressed following demethylation, as in mouse.

We also show that demethylation of genes in the postimplantation group causes their transcriptional derepression in human fibroblasts, which is the first demonstration, to the best of our knowledge, of this in a normal human cell type. Likewise, we are not aware of any previous report showing restoration of methylation at endogenous single-copy sequences (as opposed to retroviral genes) by *de novo* activity in an adult differentiated cell type. All of the genes examined were more refractory to demethylation and activation in the hTERT-1604 human fibroblasts than in the mouse NIH 3T3 fibroblasts, most likely because the latter, older cell line has become more responsive to culture conditions over time. Greater transcriptional response was seen to Aza, which inhibits all three methyltransferases, than for *DNMT1* siRNA alone, which might reflect some dependence on DNMT3A/B for maintenance in these cells as in mouse ESCs. Genes methylated postimplantation, such as *SYCP3*, lost their methylation more readily and were reactivated to a greater extent in the human cells than the testis gDMR homologues, such as *FKBP6*, which might reflect underlying differences in chromatin state between the two gene classes.

Although intragenic methylation has been reported previously for some brain genes (Lister et al., 2013; Maunakea et al., 2010; Wu et al., 2010), this is the first report, to our knowledge, to show that neuronal genes represent the major class that inherits methylation from the mother, with possible implications for transmission of neuronal phenotypes. Notably, methylation at these loci is at intragenic 'orphan' CGIs identified by CFP1 pulldown (Illingworth et al., 2010; Smallwood et al., 2011). It has been suggested that orphan CGIs can act as promoters early during development, becoming inactivated and methylated later (Illingworth et al., 2010). However, for the particular subset of orphan CGIs identified here as carrying gametic marks, 82% show no evidence of being transcriptional start sites in ESCs, this fraction rising to 89% in adult brain (Fig. 1F). Consistent with this, their demethylation resulted in no marked upregulation in steady-state mRNA levels. Recent reports suggest that intragenic methylation in somatic tissues, particularly at neuronal genes, might instead play a role in maintaining active chromatin states (Wu et al., 2010) or in splice choice (Maunakea et al., 2013). Preliminary analysis shows that this class of genes is indeed significantly enriched for alternative splicing using the DAVID ontology tool SP_PIR_KEY (46% of brain genes from the RRBS dataset, $P=2.4\times10^{-13}$, FDR=3.0×10^{-10}). Further investigation of our brain gDMR set seems warranted given the conservation of both positioning and methylation status for the promoter and intragenic CGIs of the brain genes in human.

In addition to DNMT1 (Hirasawa et al., 2008; Howell et al., 2001), ZFP57, a zinc finger-containing transcription factor, is also vital for methylation maintenance at all imprinted loci and some non-imprinted loci in preimplantation embryos and ESCs. Interestingly, *Fkbp6*, which is a testis gDMR, was also bound by ZFP57 and showed loss of methylation in KO cells (Quenneville et al., 2011). When we analysed the sites bound by ZFP57 in genome-wide ChIP studies we failed to uncover any other non-imprinted gDMRs from our study, suggesting that other factors might be involved in maintaining methylation at the other gDMR classes.

Development (2014) doi:10.1242/dev.104646

Notably, *Fkbp6* regained most methylation in 1KO+1 rescued ESCs, which express ZFP57: at the same time, it was refractive to remethylation in adult mouse and human fibroblasts, which are predicted to lack this factor. At the testis gDMR loci generally, recovery of methylation was coincident with re-establishment of transcriptional repression. These results also have important implications for the response of cells to demethylating agents.

In conclusion, we have identified two new classes of functionally significant gDMRs that appear to be evolutionarily conserved and might be important mediators of the phenotypic effects of pre- and postnatal environmental exposures that alter DNA methylation levels.

MATERIALS AND METHODS

Bioinformatic analysis and statistics

Published genome-wide methylation data from a number of studies (Borgel et al., 2010; Kobayashi et al., 2012; Smallwood et al., 2011) were re-examined using publicly available tools. Ontology analysis including statistical significance was performed in DAVID (Huang et al., 2009). Transcription marks associated with orphan CGIs were derived from Illingworth et al. (Illingworth et al., 2010). Comparison of gene features was carried out in GALAXY (Giardine et al., 2005).

All laboratory experiments were carried out in triplicate, including at least one biological repeat: graphs show a representative experiment, and error bars represent s.e.m. Statistical analysis of results was carried out in Prism (GraphPad) or Excel (Microsoft): pyrosequencing results were compared by ANOVA, RT-qPCR results were analysed by *t*-test and bisulfite clonal analysis results were compared by χ^2 test.

Mouse strains

Derivation of *Dnmt3l* knockout oocytes/ovaries and matched WT tissues was as previously described (Kaneda et al., 2004). All other mouse tissues were derived from outbred TO mice (Harlan, Huntingdon, UK). Animal work was carried out under licence from the appropriate regulatory bodies.

Cells

Culture media components are from Invitrogen unless otherwise stated. NIH 3T3 and hTERT-1604 fibroblasts were cultured in 4.5 g/l glucose D-MEM supplemented with 10% FBS and 2× NEAA. *Dnmt1* KO (± *Dnmt1*), *Dnmt3a/3b* DKO ESCs and matched WT J1 cells were a kind gift of Dr M. Okano (RIKEN Center for Developmental Biology, Kobe, Japan). ESCs were maintained on Nunc plates (Davidson & Hardy, Belfast, UK) treated with 0.1% gelatin (Sigma-Aldrich) and cultured in KnockOut D-MEM plus 15% KnockOut Serum Replacement, 1% ESC qualified FBS, 1× NEAA, 2 mM L-glutamine, 0.1 mM β-mercaptoethanol (Sigma-Aldrich) and 1000 U/ml LIF (Chemicon). For treatment with 5-aza-2′-deoxycytidine (Aza), 8×10^4 NIH 3T3 cells or 1×10^5 hTERT-1604 cells were seeded onto a 90 mm plate in complete medium and allowed to attach overnight before replacing with complete medium containing 1 μM Aza, which was renewed at 24-hour intervals up to 72 hours.

siRNA treatment

siRNA treatments were carried out in 6-well plates, each well seeded with 1×10^6 hTERT-1604 cells or 1×10^5 NIH 3T3 cells, before reverse transfection using Dharmafect 1 (Thermo Fisher Scientific) and 80 nM (NIH 3T3) or 100 nM (hTERT-1604) ON-TARGETplus SMARTpool *DNMT1* siRNA or a matched concentration of scrambled control (Thermo Fisher Scientific). Cells were cultured in complete medium to allow recovery, with extraction of RNA and DNA up to 28 days after addition of siRNA.

In situ hybridisation

In situ hybridisation was performed as previously described (Shovlin et al., 2007). Primers used to generate probes are listed in supplementary material Table S1.

Bisulfite treatment

Oocyte and sperm collection and isolation of DNA were as described (Li et al., 2004; Walsh and Bestor, 1999). DNA was extracted from NIH 3T3 and hTERT-1604 cells using the Genomic DNA Purification Kit (Fermentas). All other non-germ cell samples were incubated overnight at 55°C in lysis buffer (50 mM Tris pH 8, 0.1 M EDTA, 0.5% SDS, 0.2 mg/ml proteinase K) with rotation, and DNA was subsequently isolated by standard phenol:chloroform extraction. Total DNA from 150-200 oocytes or 200-500 ng DNA from other samples was bisulfite converted using the EpiTect Bisulfite Kit (Qiagen).

Methylation analysis

Bisulfite-treated DNA was PCR amplified in 1× buffer, 0.4 mM dNTPs, 1 μM primers (supplementary material Table S1), $MgCl_2$ at a concentration specific to the primer set and 0.01 U Taq DNA polymerase (reagents from Invitrogen). Nested PCRs and COBRA were carried out as previously described (Li et al., 2004) using *Bst*UI (*Dazl*, *Dpep3*, *Piwil1* and *Snrpn*) or *Taq*$^{\alpha}$I (*Csnka2ip*, *Fkbp6*, *H19*, *Rhox13* and *Sycp3*) enzymes from NEB. Bisulfite sequencing of cloned PCR products in pCRII-TOPO vector (Invitrogen) was performed using the ABI PRISM 3130 Genetic Analyzer (Applied Biosystems). Pyrosequencing assays are from Qiagen (supplementary material Table S2), except murine *Adcy6*, *Crocc* and *Fkbp6* and human *EFNA* and *GRIN3B*, which were all designed in house using PyroMark Assay Design software 2.0 (supplementary material Table S1). Assays were conducted using the PyroMark PCR Kit (Qiagen); conditions were: 95°C, 15 minutes; followed by 45 cycles of 94°C for 30 seconds, 56°C for 30 seconds and 72°C for 30 seconds; with final elongation at 72°C, 10 minutes. LUMA analysis was carried out as previously described (Karimi et al., 2011a).

RNA extraction and RT-PCR

RNA from all samples was extracted using the RNeasy Mini Kit (Qiagen). Reverse transcription reactions contained 300-500 ng total RNA, 0.5 μM dNTPs, 0.5 μg oligo(dT) primer, 40 U RNaseOUT (Invitrogen), 1× reverse transcriptase buffer (Fermentas) and 200 U RevertAid reverse transcriptase (Fermentas) in a total volume of 20 μl. Reaction conditions were: 42°C, 50 minutes; 70°C, 15 minutes. cDNA was stored at −20°C until use.

Each RT-PCR contained 1× buffer, 0.4 mM dNTPs, 1 μM primers (supplementary material Table S1), $MgCl_2$ at a concentration specific to the primer set and 0.01 U Taq DNA polymerase. The general PCR format was: 94°C, 3 minutes; followed by cycles of 94°C for 30 seconds, gene-specific annealing temperature for 1 minute and 72°C for 1 minute; with final elongation at 72°C, 5 minutes. RT-qPCRs were performed using 1× LightCycler 480 SYBR Green I Master (Roche), 0.5 μM primers and 1 μl cDNA. Reactions were run on the LightCycler 480 II (Roche), with an initial incubation step of 95°C, 10 minutes; followed by 50 cycles of 95°C for 10 seconds, 60°C for 10 seconds and 72°C for 10 seconds. Expression was normalised to *Hprt*, and relative expression was determined using the $\Delta\Delta C_T$ method.

Acknowledgements

We are very grateful to Masaki Okano for the gift of cells and for insightful comments. We thank Tanya Shovlin and Laszlo Hiripi for the *in situ* analysis; Hazel Mangan for oocyte material; Heather McCook, Rhonda Black, Bernie O'Doherty and Keith Thomas for technical support; and members of the C.P.W. group for comments.

Competing interests

The authors declare no competing financial interests.

Author contributions

C.E.R. made initial observations, designed assays, assembled figures and contributed to the manuscript; A.T. carried out the testis and some brain gDMR work in mouse; R.E.I. analysed brain gDMR in mouse; K.M.O. analysed human homologues and designed assays; S.S. and K.H. provided *Dnmt3l*$^{-/-}$ and WT material; C.P.W. designed and supervised the study, carried out bioinformatic analyses and wrote the manuscript.

Funding

Work in the C.P.W. laboratory was supported by grants from Invest Northern Ireland [POC206] and the Medical Research Council [MR/J007773/1]. Deposited in PMC for immediate release.

Supplementary material

Supplementary material available online at
http://dev.biologists.org/lookup/suppl/doi:10.1242/dev.104646/-/DC1

References

Bartolomei, M. S. and Ferguson-Smith, A. C. (2011). Mammalian genomic imprinting. *Cold Spring Harb. Perspect. Biol.* **3**.

Borgel, J., Guibert, S., Li, Y., Chiba, H., Schübeler, D., Sasaki, H., Forné, T. and Weber, M. (2010). Targets and dynamics of promoter DNA methylation during early mouse development. *Nat. Genet.* **42**, 1093-1100.

Chen, T., Ueda, Y., Dodge, J. E., Wang, Z. and Li, E. (2003). Establishment and maintenance of genomic methylation patterns in mouse embryonic stem cells by Dnmt3a and Dnmt3b. *Mol. Cell. Biol.* **23**, 5594-5605.

Chotalia, M., Smallwood, S. A., Ruf, N., Dawson, C., Lucifero, D., Frontera, M., James, K., Dean, W. and Kelsey, G. (2009). Transcription is required for establishment of germline methylation marks at imprinted genes. *Genes Dev.* **23**, 105-117.

Deaton, A. M. and Bird, A. (2011). CpG islands and the regulation of transcription. *Genes Dev.* **25**, 1010-1022.

DeVeale, B., van der Kooy, D. and Babak, T. (2012). Critical evaluation of imprinted gene expression by RNA-Seq: a new perspective. *PLoS Genet.* **8**, e1002600.

Giardine, B., Riemer, C., Hardison, R. C., Burhans, R., Elnitski, L., Shah, P., Zhang, Y., Blankenberg, D., Albert, I., Taylor, J. et al. (2005). Galaxy: a platform for interactive large-scale genome analysis. *Genome Res.* **15**, 1451-1455.

Gregg, C., Zhang, J., Butler, J. E., Haig, D. and Dulac, C. (2010a). Sex-specific parent-of-origin allelic expression in the mouse brain. *Science* **329**, 682-685.

Gregg, C., Zhang, J., Weissbourd, B., Luo, S., Schroth, G. P., Haig, D. and Dulac, C. (2010b). High-resolution analysis of parent-of-origin allelic expression in the mouse brain. *Science* **329**, 643-648.

Gu, T. P., Guo, F., Yang, H., Wu, H. P., Xu, G. F., Liu, W., Xie, Z. G., Shi, L., He, X., Jin, S. G. et al. (2011). The role of Tet3 DNA dioxygenase in epigenetic reprogramming by oocytes. *Nature* **477**, 606-610.

Hackett, J. A., Reddington, J. P., Nestor, C. E., Dunican, D. S., Branco, M. R., Reichmann, J., Reik, W., Surani, M. A., Adams, I. R. and Meehan, R. R. (2012). Promoter DNA methylation couples genome-defence mechanisms to epigenetic reprogramming in the mouse germline. *Development* **139**, 3623-3632.

Hirasawa, R., Chiba, H., Kaneda, M., Tajima, S., Li, E., Jaenisch, R. and Sasaki, H. (2008). Maternal and zygotic Dnmt1 are necessary and sufficient for the maintenance of DNA methylation imprints during preimplantation development. *Genes Dev.* **22**, 1607-1616.

Holm, T. M., Jackson-Grusby, L., Brambrink, T., Yamada, Y., Rideout, W. M., 3rd and Jaenisch, R. (2005). Global loss of imprinting leads to widespread tumorigenesis in adult mice. *Cancer Cell* **8**, 275-285.

Howell, C. Y., Bestor, T. H., Ding, F., Latham, K. E., Mertineit, C., Trasler, J. M. and Chaillet, J. R. (2001). Genomic imprinting disrupted by a maternal effect mutation in the Dnmt1 gene. *Cell* **104**, 829-838.

Hu, Y. G., Hirasawa, R., Hu, J. L., Hata, K., Li, C. L., Jin, Y., Chen, T., Li, E., Rigolet, M., Viegas-Péquignot, E. et al. (2008). Regulation of DNA methylation activity through Dnmt3L promoter methylation by Dnmt3 enzymes in embryonic development. *Hum. Mol. Genet.* **17**, 2654-2664.

Huang, W., Sherman, B. T. and Lempicki, R. A. (2009). Systematic and integrative analysis of large gene lists using DAVID bioinformatics resources. *Nat. Protoc.* **4**, 44-57.

Illingworth, R. S., Gruenewald-Schneider, U., Webb, S., Kerr, A. R., James, K. D., Turner, D. J., Smith, C., Harrison, D. J., Andrews, R. and Bird, A. P. (2010). Orphan CpG islands identify numerous conserved promoters in the mammalian genome. *PLoS Genet.* **6**, e1001134.

Kaneda, M., Okano, M., Hata, K., Sado, T., Tsujimoto, N., Li, E. and Sasaki, H. (2004). Essential role for de novo DNA methyltransferase Dnmt3a in paternal and maternal imprinting. *Nature* **429**, 900-903.

Karimi, M., Luttropp, K. and Ekström, T. J. (2011a). Global DNA methylation analysis using the luminometric methylation assay. *Methods Mol. Biol.* **791**, 135-144.

Karimi, M. M., Goyal, P., Maksakova, I. A., Bilenky, M., Leung, D., Tang, J. X., Shinkai, Y., Mager, D. L., Jones, S., Hirst, M. et al. (2011b). DNA methylation and SETDB1/H3K9me3 regulate predominantly distinct sets of genes, retroelements, and chimeric transcripts in mESCs. *Cell Stem Cell* **8**, 676-687.

Kobayashi, H., Sakurai, T., Imai, M., Takahashi, N., Fukuda, A., Yayoi, O., Sato, S., Nakabayashi, K., Hata, K., Sotomaru, Y. et al. (2012). Contribution of intragenic DNA methylation in mouse gametic DNA methylomes to establish oocyte-specific heritable marks. *PLoS Genet.* **8**, e1002440.

Li, E., Bestor, T. H. and Jaenisch, R. (1992). Targeted mutation of the DNA methyltransferase gene results in embryonic lethality. *Cell* **69**, 915-926.

Li, J. Y., Lees-Murdock, D. J., Xu, G. L. and Walsh, C. P. (2004). Timing of establishment of paternal methylation imprints in the mouse. *Genomics* **84**, 952-960.

Lister, R., Mukamel, E. A., Nery, J. R., Urich, M., Puddifoot, C. A., Johnson, N. D., Lucero, J., Huang, Y., Dwork, A. J., Schultz, M. D. et al. (2013). Global epigenomic reconfiguration during mammalian brain development. *Science* **341**, 1237905.

Loughery, J. E., Dunne, P. D., O'Neill, K. M., Meehan, R. R., McDaid, J. R. and Walsh, C. P. (2011). DNMT1 deficiency triggers mismatch repair defects in human cells through depletion of repair protein levels in a process involving the DNA damage response. *Hum. Mol. Genet.* **20**, 3241-3255.

Maatouk, D. M., Kellam, L. D., Mann, M. R., Lei, H., Li, E., Bartolomei, M. S. and Resnick, J. L. (2006). DNA methylation is a primary mechanism for silencing postmigratory primordial germ cell genes in both germ cell and somatic cell lineages. *Development* **133**, 3411-3418.

Maunakea, A. K., Nagarajan, R. P., Bilenky, M., Ballinger, T. J., D'Souza, C., Fouse, S. D., Johnson, B. E., Hong, C., Nielsen, C., Zhao, Y. et al. (2010). Conserved role of intragenic DNA methylation in regulating alternative promoters. *Nature* **466**, 253-257.

Maunakea, A. K., Chepelev, I., Cui, K. and Zhao, K. (2013). Intragenic DNA methylation modulates alternative splicing by recruiting MeCP2 to promote exon recognition. *Cell Res.* **23**, 1256-1269.

O'Doherty, A. M., Rutledge, C. E., Sato, S., Thakur, A., Lees-Murdock, D. J., Hata, K. and Walsh, C. P. (2011). DNA methylation plays an important role in promoter choice and protein production at the mouse Dnmt3L locus. *Dev. Biol.* **356**, 411-420.

Oda, M., Yamagiwa, A., Yamamoto, S., Nakayama, T., Tsumura, A., Sasaki, H., Nakao, K., Li, E. and Okano, M. (2006). DNA methylation regulates long-range gene silencing of an X-linked homeobox gene cluster in a lineage-specific manner. *Genes Dev.* **20**, 3382-3394.

Okano, M., Xie, S. and Li, E. (1998). Cloning and characterization of a family of novel mammalian DNA (cytosine-5) methyltransferases. *Nat. Genet.* **19**, 219-220.

Okano, M., Bell, D. W., Haber, D. A. and Li, E. (1999). DNA methyltransferases Dnmt3a and Dnmt3b are essential for de novo methylation and mammalian development. *Cell* **99**, 247-257.

Proudhon, C., Duffié, R., Ajjan, S., Cowley, M., Iranzo, J., Carbajosa, G., Saadeh, H., Holland, M. L., Oakey, R. J., Rakyan, V. K. et al. (2012). Protection against de novo methylation is instrumental in maintaining parent-of-origin methylation inherited from the gametes. *Mol. Cell* **47**, 909-920.

Quenneville, S., Verde, G., Corsinotti, A., Kapopoulou, A., Jakobsson, J., Offner, S., Baglivo, I., Pedone, P. V., Grimaldi, G., Riccio, A. et al. (2011). In embryonic stem cells, ZFP57/KAP1 recognize a methylated hexanucleotide to affect chromatin and DNA methylation of imprinting control regions. *Mol. Cell* **44**, 361-372.

Reik, W. and Walter, J. (2001). Evolution of imprinting mechanisms: the battle of the sexes begins in the zygote. *Nat. Genet.* **27**, 255-256.

Shirane, K., Toh, H., Kobayashi, H., Miura, F., Chiba, H., Ito, T., Kono, T. and Sasaki, H. (2013). Mouse oocyte methylomes at base resolution reveal genome-wide accumulation of non-CpG methylation and role of DNA methyltransferases. *PLoS Genet.* **9**, e1003439.

Shovlin, T. C., Bourc'his, D., La Salle, S., O'Doherty, A., Trasler, J. M., Bestor, T. H. and Walsh, C. P. (2007). Sex-specific promoters regulate Dnmt3L expression in mouse germ cells. *Hum. Reprod.* **22**, 457-467.

Smallwood, S. A. and Kelsey, G. (2012). De novo DNA methylation: a germ cell perspective. *Trends Genet.* **28**, 33-42.

Smallwood, S. A., Tomizawa, S., Krueger, F., Ruf, N., Carli, N., Segonds-Pichon, A., Sato, S., Hata, K., Andrews, S. R. and Kelsey, G. (2011). Dynamic CpG island methylation landscape in oocytes and preimplantation embryos. *Nat. Genet.* **43**, 811-814.

Smith, Z. D., Chan, M. M., Mikkelsen, T. S., Gu, H., Gnirke, A., Regev, A. and Meissner, A. (2012). A unique regulatory phase of DNA methylation in the early mammalian embryo. *Nature* **484**, 339-344.

Tucker, K. L., Beard, C., Dausmann, J., Jackson-Grusby, L., Laird, P. W., Lei, H., Li, E. and Jaenisch, R. (1996). Germ-line passage is required for establishment of methylation and expression patterns of imprinted but not of nonimprinted genes. *Genes Dev.* **10**, 1008-1020.

Walsh, C. P. and Bestor, T. H. (1999). Cytosine methylation and mammalian development. *Genes Dev.* **13**, 26-34.

Walsh, C. P. and Xu, G. L. (2006). Cytosine methylation and DNA repair. *Curr. Top. Microbiol. Immunol.* **301**, 283-315.

Walsh, C. P., Chaillet, J. R. and Bestor, T. H. (1998). Transcription of IAP endogenous retroviruses is constrained by cytosine methylation. *Nat. Genet.* **20**, 116-117.

Weber, M., Hellmann, I., Stadler, M. B., Ramos, L., Pääbo, S., Rebhan, M. and Schübeler, D. (2007). Distribution, silencing potential and evolutionary impact of promoter DNA methylation in the human genome. *Nat. Genet.* **39**, 457-466.

Wernig, M., Meissner, A., Foreman, R., Brambrink, T., Ku, M., Hochedlinger, K., Bernstein, B. E. and Jaenisch, R. (2007). In vitro reprogramming of fibroblasts into a pluripotent ES-cell-like state. *Nature* **448**, 318-324.

Wilkinson, L. S., Davies, W. and Isles, A. R. (2007). Genomic imprinting effects on brain development and function. *Nat. Rev. Neurosci.* **8**, 832-843.

Woodfine, K., Huddleston, J. E. and Murrell, A. (2011). Quantitative analysis of DNA methylation at all human imprinted regions reveals preservation of epigenetic stability in adult somatic tissue. *Epigenetics Chromatin* **4**, 1.

Wu, H., Coskun, V., Tao, J., Xie, W., Ge, W., Yoshikawa, K., Li, E., Zhang, Y. and Sun, Y. E. (2010). Dnmt3a-dependent nonpromoter DNA methylation facilitates transcription of neurogenic genes. *Science* **329**, 444-448.

Xu, G. L., Bestor, T. H., Bourc'his, D., Hsieh, C. L., Tommerup, N., Bugge, M., Hulten, M., Qu, X., Russo, J. J. and Viegas-Péquignot, E. (1999). Chromosome instability and immunodeficiency syndrome caused by mutations in a DNA methyltransferase gene. *Nature* **402**, 187-191.

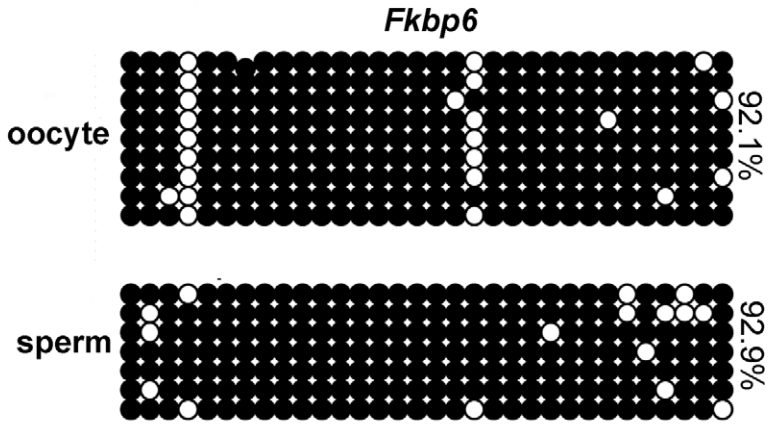

Fig. S1. Clonal analysis of methylation at *Fkbp6* in WT sperm and oocytes. Bisulphite sequencing shows that *Fkbp6* is highly methylated in oocyte as has been previously reported, but also confirms COBRA results suggesting that the gene is methylated in sperm collected from cauda epididymis.

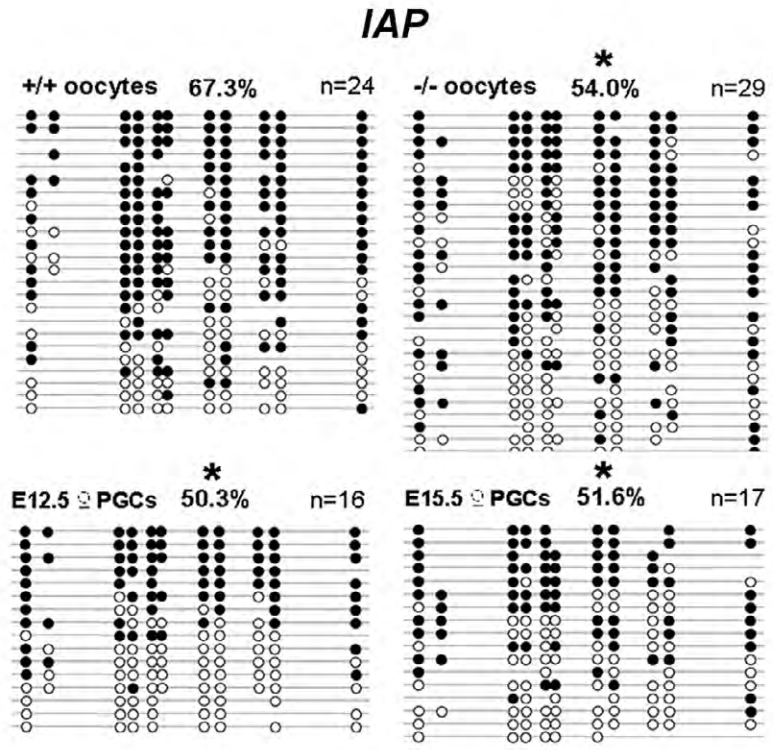

Fig. S2. Clonal analysis of methylation at IAP in WT primordial germ cells, WT oocytes and *Dnmt3l*$^{-/-}$ oocytes. Bisulphite sequencing shows that loss of DNMT3L from murine oocytes causes the methylation of IAP sequences to be reduced to a level comparable to that seen during methylation reprogramming in female PGCs at embryonic day (E) 12.5 and E15.5. WT and *Dnmt3L* KO oocytes indicated by +/+ and −/−, respectively. Asterisk denotes a significant difference in methylation (P<0.05) compared to +/+ sample, as determined by Chi-squared test. The number of sequences analysed for each sample is indicated.

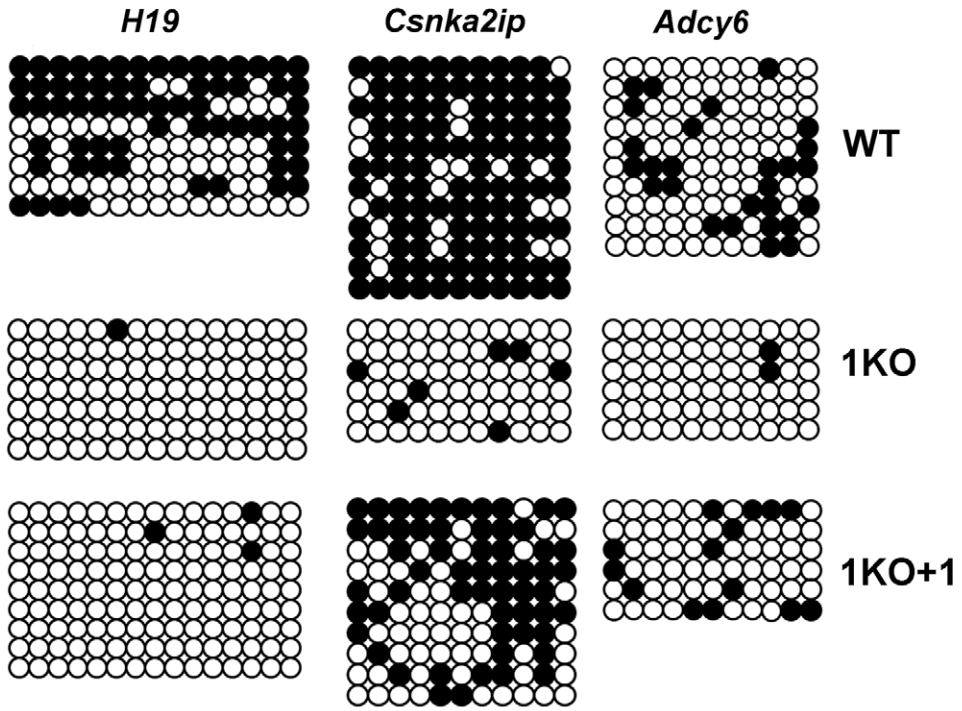

Fig. S3. Additional bisulphite sequencing data indicating methylation rescue on non-imprinted genes. Genes from each group (*H19*- imprinted; *Csnka2ip* –testis; *Adcy6*- brain) were analysed in WT ES cells, cells lacking DNMT1 (1KO) and 1KO cells rescued with an expression construct carrying Dnmt1 (1KO+1).

Table S1. Primers used for analysis of transcription and methylation levels

Application	Oligo sequence
RT-PCR	
ACTB-F	5'-gga ctt cga gca aga gat gg-3'
ACTB-R	5'-agc act gtg ttg gcg tac ag-3'
Adcy6-F	5'-gag atg gct tcg atc atg tc-3'
*Adcy*6-R	5'-cac tgt ctg agg atc aag atc-3'
Csnka2ip-F	5'-tca gct acg atc aat tca tcc-3'
Csnka2ip-R	5'-agg acg agg gtt tgg ctt tcc-3'
DAZL-F	5'-cgt gga tgt gca gaa gat ag-3'
DAZL-R	5'-aac tgt ggt gga gga gga tg-3'
Dpep3-F	5'-tgc agt ctg ttt gct aac gt-3'
Dpep3-R	5'-ggt atg tag ata cat cct cc-3'
DPEP3-F	5'-ttg acc tca ttc acc gca tg-3'
DPEP3-R	5'-tgt act gca ggt gaa ggt aag-3'
Fkbp6-F	5'-gtt cct gtt caa gcc agc ct-3'
Fkbp6-R	5'-ctg aga gtg cac aga act tg-3'
FKBP6-F	5'-gat cag cac ccc ctg aag ag-3'
FKBP6-R	5'-tct cct gct gta gaa cca tc-3'
Grin3b-F	5'-tcc tgg cag ctg cca cag ag-3'
Grin3b-R	5'-aga gca cta gag caa tgt cc-3'
Hprt-F	5'-gga gat gat ctc tca act tt-3'
Hprt-R	5'-cca aca aca aac ttg tct gg-3'
IAP-F	5'-caa agg ctt aca aga ctg gc-3'
IAP-R	5'-tgt cct ctg atc att tct gc-3'
Piwil1-F	5'-aga ctt cag aac cct ctt cc-3'
Piwil1-R	5'-gat gac att gta gtg tgt tgg-3'
PIWIL1-F	5'-cct ggc ttc act act tcc atc-3'
PIWIL1-R	5'-cca gtc aat atc atc cac tct g-3'
Rhox13-F	5'-ccg gaa tct gaa tag cag cg-3'
Rhox13-R	5-'acg aga gtg atg acg act cg-3'
RHOXF1-F	5'-gaa gtt cac gct gtt gca gg-3'
RHOXF1-R	5'-ctg atg tcg cct aca tct gg-3'
SYCP1-F	5'-cgt acc acc gag atc aag cag c-3'
SYCP1-R	5'-cct tcc tga tag tga cag tc-3'
Sycp3-F	5'-aat ctg gga agc cac ctt tg-3'
Sycp3-R	5'-ctt caa tta tcc cag cag atc-3'
SYCP3-F	5'-tct ggg aag ccg tct gtg ga-3'
SYCP3-R	5'-cca gca tat tct gca ctt cac ccc c-3'
TEX12-F	5'-tct cca gtg cca gat agt cc-3'
TEX12-R	5'-gca tct act gct gct ctc tc-3'
Tssk2-F	5'-gga tgg aag aca ggc tgg ctg-3'
Tssk2-R	5'-ctt gtt cct tgc acc tgt gcc-3'

RT-qPCR	
Adcy6-F	5’-gag atg gct tcg atc atg tc-3’
Adcy6-R	5’-cac tgt ctg agg atc aag atc-3’
Crocc-F	5’-gcg gag cgc agg ccg cta g-3’
Crocc-R	5’-agc ctg gag ctg agg ctg gag-3’
DAZL	Sequences as for RT-PCR
Dnmt1-F	5’-ggctttccagatagctaccg-3’
Dnmt1-R	5’-gcaggcagagcttaatctcc-3’
Dnmt3l-F	5’-ctc atc cct acc tac ggg ttc-3’
Dnmt3l-R	5’-cag tct tcc agt acc aca tcc-3’
Dpep3	Sequences as for RT-PCR
DPEP3	Sequences as for RT-PCR
Efna2-F	5’-cag cga ggc ttc aag cgc tg-3’
Efna2-R	5’-gag gtt ggg agg tgt ggc ag-3’
Fkbp6	Sequences as for RT-PCR
FKBP6	Sequences as for RT-PCR
Ggn1-F	5’-aag tgc tac tgc cgc cat caa c-3’
Ggn1-R	5’-gca agt cgt agt gct cca gg-3’
Grin3b-F	5’-tcc tgg cag ctg cca cag ag-3’
Grin3b-R	5’-aga gca cta gag caa tgt cc-3’
HPRT-F	5’-agc cct ggc gtc gtg att agt-3’
HPRT-R	5’-ccc gtt gag cac aca gag gcc ta-3’
IAP	Sequences as for RT-PCR
Piwil1	Sequences as for RT-PCR
PIWIL1	Sequences as for RT-PCR
Rhox9-F	5’-cga gga tga caa cat cca gg-3’
Rhox9-R	5’-tgg gga agc gat tct ctt gg-3’
Rhox13	Sequences as for RT-PCR
RHOXF1-F	5’-cta ctg cct gag tgt ata cc-3’
RHOXF1-R	5’-tca tgc cgt tct cgt ggt tc-3’
Snrpn-F	5’-tgc tac gtg ggg aga act tg-3’
Snrpn-R	5’-cct ggg gaa tag gta cac ctg-3’
Spag12-F	5’-tta caa tcc tgg atg cag tc-3’
Spag12-R	5’-att cgc aga ggc agc cgc cga a-3’
Spata16-F	5’-gca gca gga cag ttc agg ac-3’
Spata16-R	5’-cgt agg tag cat gtg acg agc-3’
SYCP1	Sequences as for RT-PCR
Sycp3	Sequences as for RT-PCR
SYCP3	Sequences as for RT-PCR
Syt2-F	5’-gga gcc aaa tgt ggc tcc ggc-3’
Syt2-R	5’-cac agc cat ggc gat cag ag-3’
Tbpl1-F	5’-aac cgg aag tga gtg gct ag-3’
Tbpl1-R	5’-gcg tcg gac gcggag aag aa-3'
TEX12	Sequences as for RT-PCR
Trim52-F	5’-taa gat ggc cac ctc tac ac-3’

Trim52-R	5’-ccg gtc ctg ctc atc ttc ct-3’
COBRA and bisulfite sequencing	
Csnka2ip-outer-F	5’-tga tat ttt ttg att tga ggg-3’
Csnka2ip-outer-R	5’-ccc taa ata tca tct aaa cta cac ct-3’
Csnka2ip-inner-F	5’-gag gtt ttt gtt tgt tat tga gtg aag-3’
Csnka2ip-inner-R	5’-atc taa atc aca aaa aaa ttc cac a-3’
Dazl-outer-F	5’-taa ttt ttt agt gtt ggt gta gg-3’
Dazl-outer-R	5’-taa atc ccc taa ccc cc-3’
Dazl-inner-F	5’-gtt tta ttt tgg ggg ttg-3’
Dazl-inner-R	5’-aaa ctc tct ttc cac cac-3’
Dpep3-outer-F	5’-gtg tta tta gga atg ttt gga g-3’
Dpep3-outer-R	5’-cac taa cac aca taa atc taa cca-3’
Dpep3-inner-F	5’-gga gta gtt agg gtg tag gtt att-3’
Dpep3-inner-R	5’-att tct aac cac taa caa acc c-3’
Fkbp6-outer-F	5’-tat agg ttt tag agg tgg aag t-3’
Fkbp6-outer-R	5’-cca aac ata aca tta aaa cca-3’
Fkbp6-inner-F	5’-ggg tgt ttg tta ttt atg gt-3’
Fkbp6-inner-R	5-cca aaa ctc cat cat cct act tta c-3’
Grin3b-outer-F	5’-gtg gaa ggt att ggg gag tat tag-3’
Grin3b-outer-R	5’-cct cct aac tct tca tcc aaa taa a-3’
Grin3b-inner-F	5’- ttt aga ggg att tta ggg tta gg-3’
Grin3b-inner-R	5’- aca act cta act ccc cta cca c-3’
H19-outer-F	5’-gag tat tta gga ggt ata aga att-3’
H19-outer-R	5’-atc aaa aac taa cat aaa ccc ct-3’
H19-inner-F	5’-gta agg aga tta tgt tta ttt ttg g-3’
H19-inner-R	5’-cct cat taa tcc cat aac tat-3’
IAP-F	5’-ttg ata gtt gtg ttt taa gtg gta aat aaa-3’
IAP-R	5’-caa aaa aaa cac cac aaa cca aaa t-3’
Piwil1-outer-F	5’-ggg tgg att tgt ata gtt gtt t-3’
Piwil1-outer-R	5’-tcc aat cct atc cta acc cc-3’
Piwil1-inner-F	5’-tgt agt ggg ttt tgg tat agg g-3’
Piwil1-inner-R	5’-acc ccc tac aac aaa ctt ctc-3’
Rhox13-outer-F	5’-agt ggg tag aaa gtt att ggt agt t-3’
Rhox13-outer-R	5’-cct cct caa aat cta aaa tat cct-3’
Rhox13-inner-F	5’-att att ttg agg gga gtg tg-3’
Rhox13-inner-R	5’-cac aac cta taa ctc ctc cac t-3’
Snrpn-outer-F	5’-tat gta ata tga tat agt tta gaa att ag-3’
Snrpn-outer-R	5’-aat aaa ccc aaa tct aaa ata ttt taa tc-3’
Snrpn-inner-F	5’-aat ttg tgt gat gtt tgt aat tat ttg g-3’
Snrpn-inner-R	5’-ata aaa tac act ttc act act aaa atc c-3’
Sycp3-outer-F	5’-agt aaa gat ggt tag gtt agg tgg-3’
Sycp3-outer-R	5’-aac cta acc cca att cct tc-3’
Sycp3-inner-F	5’-gtg agg tgt tta tta tgg aag tg-3’
Sycp3-inner-R	5’-cca act tcc tac cta aat acc c-3’

Pyrosequencing	
Adcy6-F	5'-tgt ttt ggt tta ttt gga aga agt-3'
Adcy6-R*(biotinylated)*	5'-act tat aca aat att cca atc taa aca att-3'
Adcy6-seq	5'-ggt tta ttt gga aga agt at-3'
Crocc-F	5'-ttt gtg tag ggt tga gtg g-3'
Crocc-R*(biotinylated)*	5'-ccc aaa act acc cta tct aac ac-3'
Crocc-seq	5'-gtt ggg gat agg ttt-3'
EFNA-F	5'-tgg agg tga gta tta atg att att t-3'
EFNA-R*(biotinylated)*	5'-acc cca ctc aca aat ata at-3'
EFNA-seq	5'-gtg agt att aat gat tat ttg gat-3'
Fkbp6-F	5'-tgg ttt tag tta tta att ttg tag taa tgt-3'
Fkbp6-R*(biotinylated)*	5'-aca act atc tcc aaa aac ctt ac-3'
Fkbp6-seq	5'-gtg ttt tgt ttt tgt gat aga-3'
Piwil1-F	5'-att tgg tag ttg ggg ttg tt-3'
Piwil1-R(biotinylated)	5'-ccc cct aca aca aac ttc tc-3'
Piwil1-seq	5'-ggt agt tgg ggt tgt ta-3'
GRIN3B-F	5'-agg ttt ttt agg ggt ttg tta t-3'
GRIN3B-R*(biotinylated)*	5'-ata cta caa cct act ccc ctt ac-3'
GRIN3B-seq	5'-aga ttt tgt aga tga gta ttt att-3'
In situ hybridisation	
Ddx4	Toyooka et al. (2000)
Fkbp6-F	5'-atg gac aag cct ttc gat tct-3'
Fkbp6-R	5'- ctg aag atc tgc ttc cac agg-3'

Toyooka, Y., Tsunekawa, N., Takahashi, Y., Matsui, Y., Satoh, M. and Noce, T. (2000). Expression and intracellular localization of mouse Vasa-homologue protein during germ cell development. Mech. Dev. 93, 139-149.

Table S2. Commercially available methylation pyrosequencing assays used

Gene	***Assay number***
ADCY6	PM00160440
Dazl	PM00291270
DAZL	PM00013636
DPEP3	PM00175077
FKBP6	PM00028973
Grin3b	PM00217091
Peg1	PM00384230
PIWIL1	PM00051884
Rhox13	PM00434042
SNRPN	PM00168252
Sycp3	PM00219744
SYCP3	PM00052514
Sycp1	PM 00337001